Available online at www.sciencedirect.com
ScienceDirect
Catalysis Today 129 (2007) 407–413
CATALYSIS TODAY
www.elsevier.com/locate/cattod

Effects of divalent metal ion (Mg^{2+}, Zn^{2+} and Be^{2+}) doping on photocatalytic activity of ruthenium oxide-loaded gallium nitride for water splitting

Naoki Arai [a], Nobuo Saito [a], Hiroshi Nishiyama [a], Kazunari Domen [b], Hisayoshi Kobayashi [d], Kazunori Sato [c], Yasunobu Inoue [a,*]

[a] *Department of Chemistry, Nagaoka University of Technology, Japan*
[b] *Department of Chemical System Engineering, School of Engineering, The University of Tokyo, Japan*
[c] *Department of Environment Engineering, Nagaoka University of Technology, Japan*
[d] *Department of Chemistry and Materials Technology, Kyoto Institute of Technology, Japan*

Available online 27 September 2007

Abstract

The effects of divalent metal ion doping on the photocatalytic activity of GaN powder for overall water splitting were studied. The doping of Zn^{2+}, Mg^{2+} and Be^{2+} to GaN converted it to be a remarkably active and stable photocatalyst in the presence of RuO_2 as a co-catalyst. Both H_2 and O_2 were produced from the initial stage of UV light illumination, and the ratio of H_2 to O_2 attained at the stoichiometric ratio of 2.0 at stationary conditions. Main absorption of undoped GaN was at around 390 nm, and a slight shift to longer wavelength occurred with the divalent metal ion-doped GaN. Undoped GaN showed photoluminescence peak due to band gap transition, whereas Zn^{2+} and Mg^{2+}-doped GaN generated a broad photoluminescence peak having a center at around 450 nm and a tail extending to 600 nm. In RuO_2-dispersed Mg^{2+}-doped GaN, with increasing content of Mg in starting materials used for preparation, the activity increased, whereas photoluminescence intensity decreased. The role of divalent metal ion dopants is concluded to produce p-type GaN, which is able to increase the concentration and mobility of holes.

Keywords: Divalent metal ion doping; Photocatalytic activity; Water splitting; GaN powder

1. Introduction

In view of current interest of solar energy conversion to hydrogen as alternative and renewable energy sources, the development of new kinds of photocatalysts for overall water splitting is an attractive and important subject. One group of the photocatalysts so far developed has been transition metal oxides involving Ti^{4+}, Zr^{4+}, Nb^{5+}, Ta^{5+} and W^{6+} ions with d^0 electronic configuration [1–7]. The other has been typical metal oxides involving Ga^{3+}, In^{3+}, Ge^{4+}, Sn^{4+} and Sb^{5+} ions with d^{10} electronic configuration [8–15]. For both groups, NiO_x or RuO_2 was mostly used as a co-catalyst. Generally, metal oxide photocatalysts have wide band gaps because of deep O2p valence bands. Thus, recent photocatalyst research for water decomposition has shifted from metal oxides to oxynitrides and metal nitrides in the expectation of establishment of narrow band gap photocatalysts, since the potential of N2p orbital is higher than that of O2p orbital.

We have paid attention to metal nitrides with d^{10} electronic configuration and have shown that β-Ge_3N_4 became a strong photocatalyst for overall water splitting to produce H_2 and O_2 when RuO_2 was dispersed on the nitride surface as a co-catalyst[16]. β-Ge_3N_4 was the first example of a photocatalytically active d^{10}-metal nitride. As the next step, we have focused on gallium nitride, GaN, with d^{10} electronic configuration. GaN has been used extensively for application in laser and light-emitting diodes as semiconductor materials. However, GaN itself showed poor activity for water splitting even in the presence of RuO_2 [17]. In an attempt to activate GaN, the formation of a solid solution of GaN with ZnO ($Ga_{1-x}Zn_x$)($N_{1-x}O_x$), has been found to convert GaN to be photocatalytically active for water splitting when combined with RuO_2 and also to extend light absorption

* Corresponding author. Tel.: +81 258 47 9832; fax: +81 258 479 830.
E-mail address: inoue@analysis.nagaokaut.ac.jp (Y. Inoue).

0920-5861/$ – see front matter
doi:10.1016/j.cattod.2006.08.072

region from 400 to 500 nm. In fact, the wavelength dependence of activity showed an ability of splitting water to H_2 and O_2 at 500 nm when RuO_2 or Cr_2O_3-Rh_2O_3 was dispersed on the surface[18,19]. Thus, one approach to activating GaN for water splitting is to make the solid solution of GaN and ZnO. For the availability of metal nitrides as a photocatalyst for water splitting, it is useful to find out different methods of activating GaN.

For the control of optical and electronic properties, the divalent and tetravalent metal ion doping to GaN, forming p-type and n-type GaN, have been used, respectively. This offers a possibility of activating GaN, and we have reported in a previous paper that RuO_2-dispersed divalent metal ions (Zn^{2+} and Mg^{2+})-doped GaN became stable photocatalysts for overall water splitting, whereas RuO_2-dispersed tetravalent metal ions (Si^{4+} and Ge^{4+})-doped GaN showed little photocatalytic activity [17]. The results that the dopants converted GaN to be an active photocatalyst are quite interesting. The present study was undertaken to investigate the effects of divalent metal ion dopants on photocatalytic properties of GaN in detail and to reveal an activation mechanism. The effects of Be^{2+}-doping to GaN, in addition to Zn^{2+} and Mg^{2+} doping and the influences of preparation conditions on photocatalytic properties and photoluminescence were investigated. The band structures of GaN were calculated by a DFT method to understand the electronic structures.

2. Experimental

Nitridation was performed in a NH_3 flow at 1273 K for 15 h using a rotary kiln-type electric furnace fabricated in-house[17]. Undoped GaN was synthesized by nitridation of Ga_2S_3 (High Purity Chemicals, 99.99%). Zn^{2+}-doped GaN was prepared from a mixture of Ga_2S_3 and ZnS (High Purity Chemicals, 99.999%) with a molar ratio of Ga:Zn = 1:2 in a starting material. Be^{2+}-doped GaN was obtained from a mixture of Ga_2S_3 and BeO (High Purity Chemicals, 99%) with a molar ratio of Be/(Ga + Be) = 0.03. For Mg^{2+}-doped GaN, the different ratios of Ga_2S_3 and MgS (High Purity Chemicals, 99.99%) with a molar ratio of Mg/(Ga + Mg) = 0.005, 0.01, 0.03, 0.05 and 0.07 were used as starting materials. As the different preparation of Mg^{2+}-doped GaN, a coprecipitate was first prepared by a dropwise addition of NH_3 aqeous to an aqueous solution of $Ga(NO_3)_3$ (High Purity Chemicals, 99.9%) and $Mg(NO_3)_2$ (High Purity Chemicals, 99%), followed by quick oxidation at 1073 K for 2 min. The prepared Mg-doped Ga_2O_3 was subjected to nitridation at 1273 K for 15 h (this will be referred to as Mg^{2+}-doped GaN(N)). The GaN was characterized by means of an X-ray diffraction method (XRD: Rigaku RAD-3A), scanning electron microscopy (SEM: Shimadzu EPMA-1600), UV-diffuse reflectance spectroscopy (UV-DRS: Jasco V-560), and photoluminescence spectroscopy (PLS: Jasco FP-6500). For SEM images, 50 nm of Au thin film was deposited on the nitride surface. In UV-DRS, reflection spectra were obtained using a standard reflective sample and converted to absorbance by the Kubelka–Munk method. The photoluminescence spectra were recorded in air at room temperature.

To deposit co-catalyst RuO_2, undoped and doped GaN were impregnated up to incipient wetness with $Ru_3(CO)_{12}$ in THF solution, dried at 333 K and calcined in air at 623 K to convert the Ru carbonyl to RuO_2. The RuO_2 loading was 3.5 wt% as a metal base. The photocatalytic overall water splitting reaction was carried out in a gas-circulating closed system equipped with an inner irradiation-type Pyrex glass reaction cell. A photocatalyst (0.8 g) was introduced to distilled and ion-exchanged water (700 ml). Prior to photocatalytic run, dissolved gases in water were degassed by evacuation, and then 4 kPa of Ar gas was introduced and circulated with a piston pump. The photocatalyst was dispersed by stirring with a magnet rotator during reaction and was illuminated by a 450 W high pressure mercury lamp (USHIO UM-452). The evolved gases were analyzed by a gas chromatograph directly connected to the reaction system.

The electronic band structure of GaN was calculated using a planewave-based DFT program, CASTEP. The fundamental unit cell of GaN was formed by two Ga atoms and two N atoms. The kinetic cut-off energy was set to 280.0 eV.

3. Results

Fig. 1 shows photocatalytic water splitting on RuO_2-dispersed Mg^{2+}-doped GaN(N), Zn^{2+}-doped GaN and Be^{2+}-doped GaN under light irradiation. Without doping of the divalent metal ions, the activity of GaN itself was extremely small in RuO_2 loading. However, for three kinds of the divalent metal ion-doped GaN, light irradiation produced H_2 and O_2 starting with an initial stage of reaction, and the products increased with irradiation time. As shown in Fig 1(a), the activity of Mg^{2+}-doped GaN(N) for H_2 and O_2 production increased with repeating run and leveled off after the 3rd run. At the 4th run, the ratio of H_2 to O_2 was nearly the stoichiometric value of 2.0. A small amount of nitrogen was produced until the second run, after which little N_2 evolution occurred. The behavior of activity increase with repeating run in initial stages was observed for Mg^{2+}-doped GaN, as reported previously. Fig. 1(b) shows the reaction on Zn^{2+}-doped GaN. The production of H_2 and O_2 in proportion to irradiation time occurred from the first run, and the activity was nearly stable with run. The ratio of H_2 to O_2 was approximately 2.0 at the third run, and little evolution of N_2 occurred in repeated run. For Be^{2+}-doped GaN, H_2 and O_2 production decreased up to the third run, and became constant after third run (Fig. 1(c)). The ratio H_2 to O_2 was approximately 2.0. The stable activity for H_2 evolution was 0.45, 0.18 and 0.38 mmol h^{-1} for Mg^{2+}-doped GaN(N), Zn^{2+}-doped GaN and Be^{2+}-doped GaN. The previously reported activity for Mg^{2+}-doped GaN was 0.65 mmol h^{-1}. Thus, the activation effect of the divalent metal ions doped was larger in the order of $Mg^{2+} > Be^{2+} > Zn^{2+}$. The total amounts of H_2 produced in the irradiation were 4.80, 1.75, and 5.03 mmol for Mg^{2+}-doped GaN(N), Zn^{2+}-doped GaN and Be^{2+}-doped GaN, respectively. These amounts were larger by a factor of 280 for Mg^{2+}-doped GaN(N), and by a factor of 102 for Be^{2+}-doped GaN, and by a factor of 293 for Zn^{2+}-doped GaN than the estimated amount of

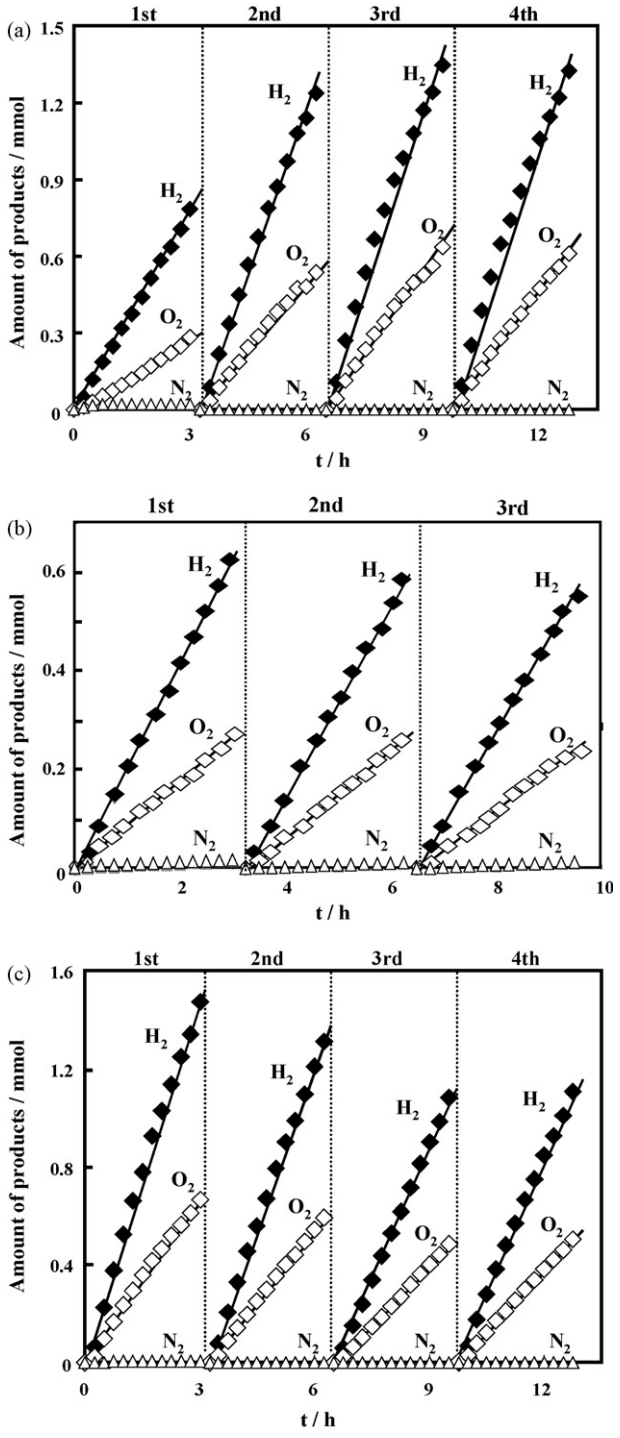

Fig. 1. Overall water splitting to H_2 and O_2 on Mg^{2+}-doped GaN(N) (a), Zn^{2+}-doped GaN (b), and Be^{2+}-doped GaN (c). RuO_2-loading was 3.5 wt%. (◆) H_2; (◇) O_2; (△) N_2.

Ga^{3+} ion present at the GaN surface. In the repeating run, the evolution of N_2 decreased dramatically in the second and third run, gradually with further repeating run, and lowered to an extremely low level. The total amounts of N_2 evolved were 240–340 times lower than that of H_2 in all cases. In GaN doped by different amount of Mg^{2+}, the photocatalytic activity was stable independent of the amount of Mg^{2+} doped, but the amount of N_2 evolved decreased with increasing $Mg^{2+}$and

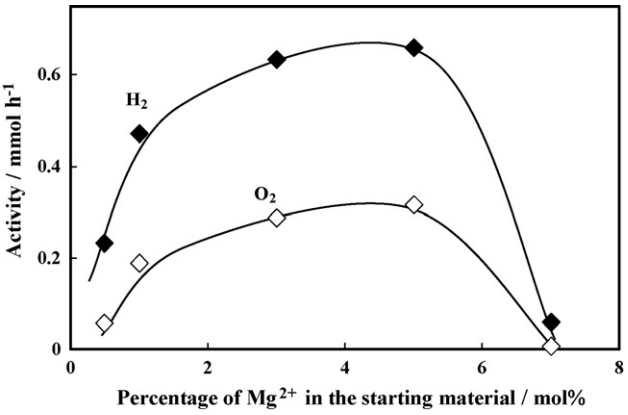

Fig. 2. Photocatalytic activity for overall water splitting on Mg^{2+}-doped GaN as a function of Mg^{2+} content in the mixture of starting material. RuO_2-loading, 3.5 wt%. (◆) H_2; (◇) O_2.

became the lowest at 5 mol% Mg^{2+}, at which the photocatalytic activity became the highest. The results indicate the divalent metal ion-doped GaN became an efficient and stable photocatalyst for the overall water splitting by loading RuO_2 as a co-catalyst.

Fig. 2 shows photocatalytic activity as a function of Mg^{2+} content in the starting material. Both H_2 and O_2 evolutions increased sharply by the addition of Mg^{2+}, increased considerably with increasing Mg^{2+} content, reached the highest level at around 5 mol%, above which the activity decreased sharply. Fig. 3 shows SEM images of undoped, Zn^{2+}- and Mg^{2+}-doped GaN. The three GaN powders exhibited similar particles having irregular forms with sharp-corner. Particle sizes were in the range of 1–4 μm. The surface morphology remained nearly unchanged with doping.

Fig. 4 shows XRD patterns of undoped GaN, Zn^{2+}-doped GaN, Mg^{2+}-doped GaN, Be^{2+}-doped GaN and Mg^{2+}-doped GaN(N). All the samples exhibited single-phase diffraction patterns characteristic of a wurtzite structure. No significant changes in the diffraction peak positions were observed, but the intensity of three major diffraction peaks due to 1 0 0, 0 0 2 and 1 0 1 were slightly different between two GaN (undoped GaN and Be^{2+}-doped GaN) and three GaN (Zn^{2+}-doped GaN, Mg^{2+}-doped GaN, and Mg^{2+}doped GaN(N)). In the former group, the intensity of 0 0 2 peak was nearly the same as or slightly larger than that of 1 0 0 peak, whereas in the latter, the intensity of 0 0 2 peak was considerably lower than that of 1 0 0 peak.

Fig. 5 shows UV–vis diffuse reflectance spectra of undoped GaN, Zn^{2+}-doped GaN, Mg^{2+}-doped GaN, Be^{2+}-doped GaN and Mg^{2+}-doped GaN (N). The absorption of undoped GaN occurred at around 390 nm, increased sharply with shorter wavelength, and leveled off at 370 nm. This coincides with a reported band gap of approximately 3.4 eV. The absorption threshold of the Zn^{2+}-doped GaN considerably shifted to longer wavelength, and the absorption leveled off at around 375 nm. The red shifts of absorption threshold were also observed for Mg^{2+} and Be^{2+} doped GaN, but the extent of shifts were smaller than that of the Zn^{2+}-doped GaN. The absorption characteristics was similar between Mg^{2+}-doped GaN and Mg^{2+}-doped GaN(N), independent of preparation of GaN.

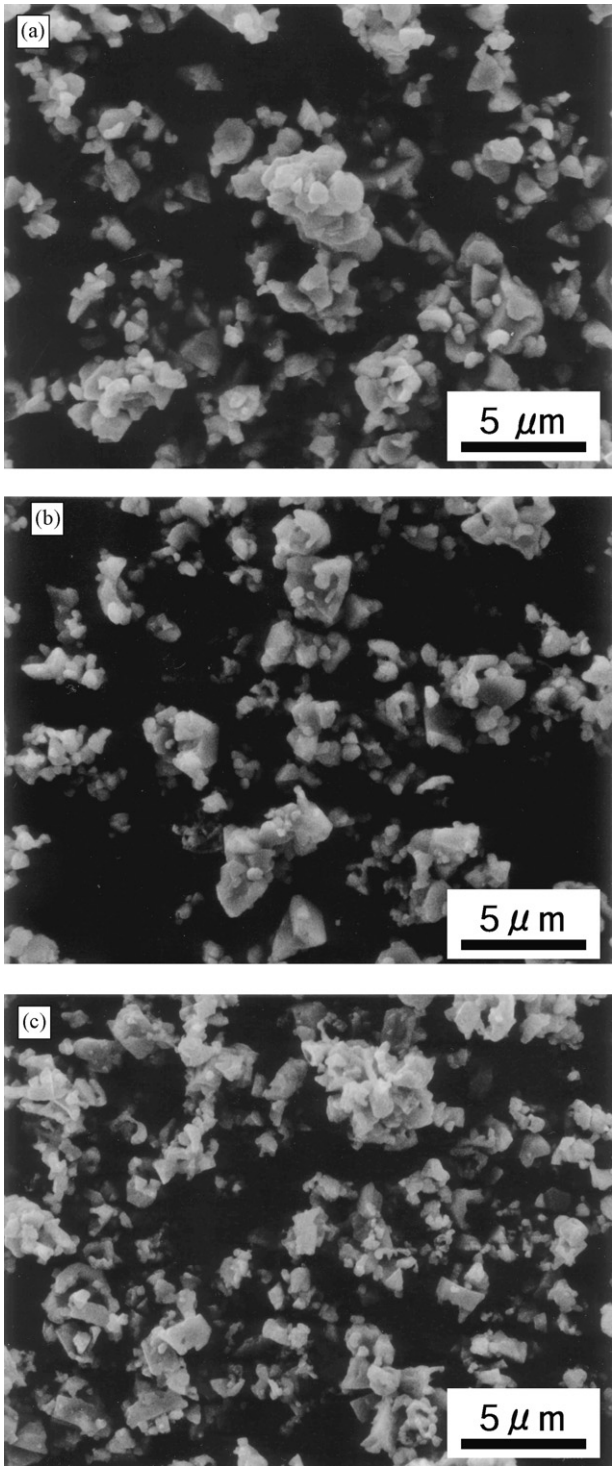

Fig. 3. SEM images of undoped GaN (a), Zn^{2+}-doped GaN (b), and Mg^{2+}-doped GaN (c).

Fig. 6 shows the photoluminescence spectra of various Mg^{2+}-doped GaN prepared from different Mg contents in a mixture of the starting material. The figure also shows spectrum for undoped GaN for comparison. The photoluminescence of undoped GaN showed a sharp peak at around 373 nm with an excitation wavelength of 330 nm. Mg^{2+}-doped GaN exhibited a broad emission spectrum having a maximum at around 450 nm

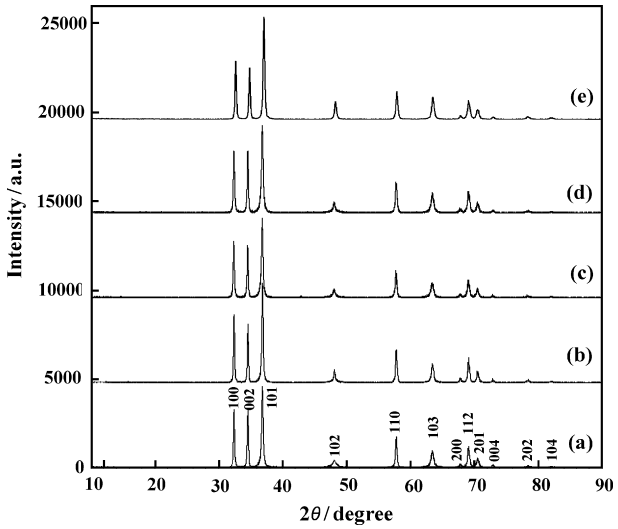

Fig. 4. XRD patterns of undoped GaN (a), Zn^{2+}-doped GaN (b), Mg^{2+}-doped GaN (c), Be^{2+}-doped GaN (d), and Mg^{2+}-doped GaN(N) (e).

and a tail extending to 600 nm. The highest emission intensity occurred when the molar ratio of Mg/(Ga + Mg) in the mixture was 0.005. With an increase in the ratio of Mg, the intensity decreased with a shift of the center position to longer wavelength. The intensity became negligible at Mg/(Ga + Mg) = 0.07. Mg^{2+}-doped GaN (N) showed photoluminescence similar to that of Mg^{2+}-doped GaN, but its intensity was slightly stronger than that of Mg^{2+}-doped GaN. The emission pattern of Zn^{2+}-doped GaN was analogous to that of Mg^{2+}-doped GaN, although its intensity was twice larger than that of the latter.

Fig. 7 shows the density of states of GaN obtained by DFT calculation. The N2s and Ga3d orbitals were located in the inner level. The lower and upper part of valence band was composed of N2p mixed with Ga4p and Ga4s orbital, respectively. The conduction band consisted of hybridized Ge4s4p mixed with N2p orbital. Fig. 8 shows the contour map

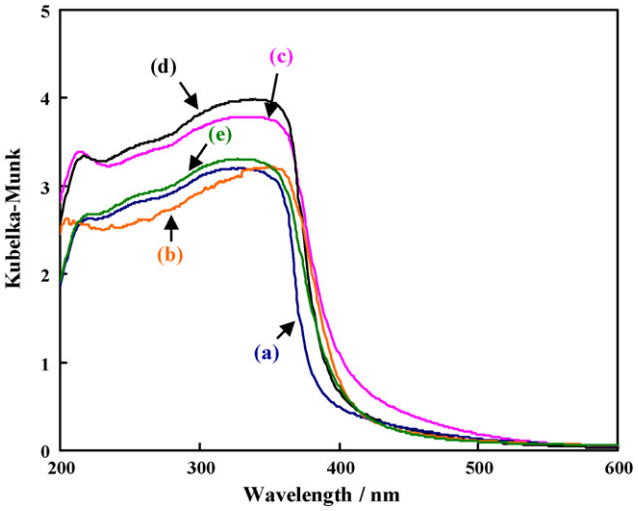

Fig. 5. UV–visible diffuse reflectance spectra of undoped GaN (a), Zn^{2+}-doped GaN (b), Mg^{2+}-doped GaN (c), Be^{2+}-doped GaN (d), and Mg^{2+}-doped GaN(N) (e).

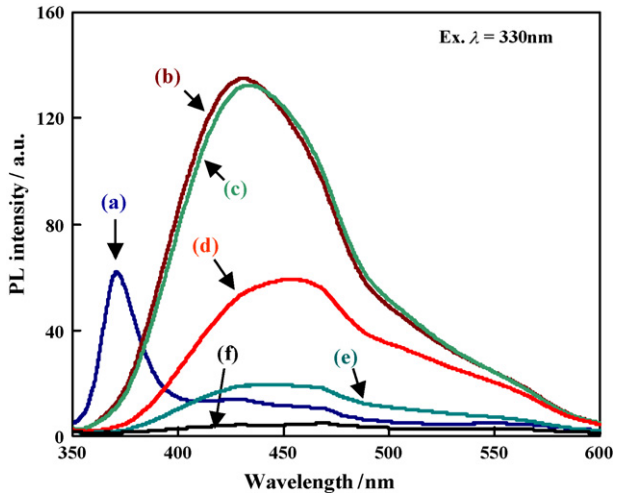

Fig. 6. Changes in photoluminescence spectra of Mg^{2+}-doped GaN with Mg^{2+} content in the mixture of starting materials. Measurement = room temperature; excitation wavelength = 330 nm. Mg/(Mg + Ga) = 0 (a), 0.005 (b), 0.01 (c), 0.03 (d), 0.05 (e), and 0.07 (f).

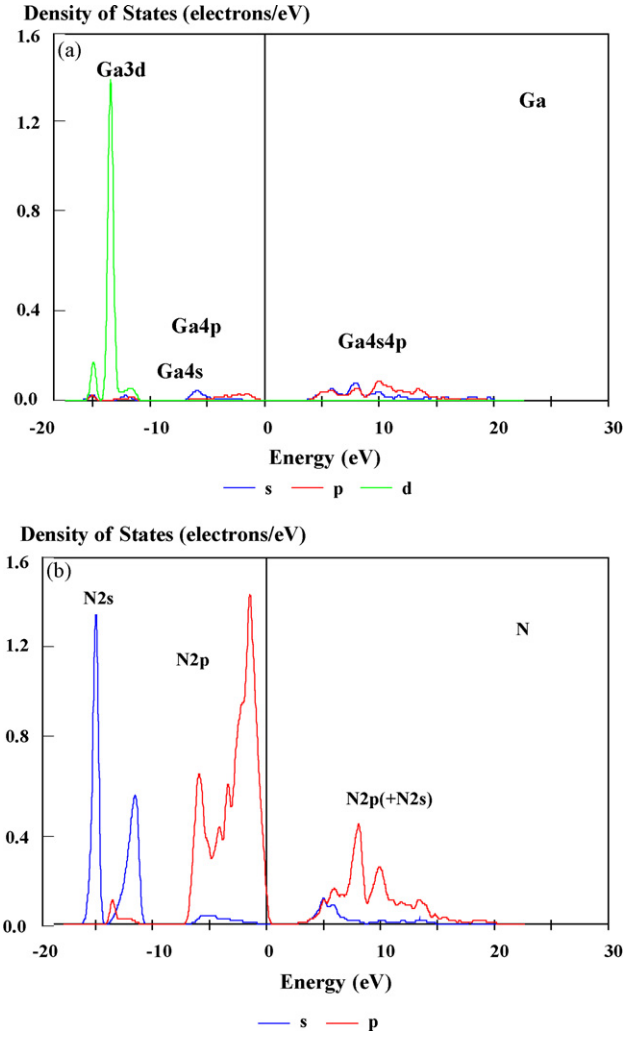

Fig. 7. Partial density of states for Ga atom (a) and N atom (b) of GaN.

of HOMO and LUMO. The results clearly show that the HOMO level was formed by N2p orbital, whereas the LUMO level by Ga4s4p mixed with N2p. The band gap was calculated to be 2.57 eV.

4. Discussion

Undoped GaN produced a small amount of hydrogen without O_2 when RuO_2 was used as a co-catalyst. On the other hand, Mg^{2+}-, Zn^{2+}- and Be^{2+}-doped GaN showed marked and stable photocatalytic activity with a sotichiometric production of H_2 and O_2. Turnover number was as large as two orders of magnitudes. The results indicate that the doping of divalent metal ion converted poorly active GaN to be an efficient photocatalyst. In the preparation of Zn^{2+}-doped GaN, a large amount of ZnS (Ga:Zn molar ratio = 1:2) was used in a starting mixture, since Zn metal produced from ZnS in a reducing atmosphere of NH_3 readily evaporated during nitridation. The EPMA analysis showed that Zn content doped in GaN was around 0.05 mol%. This indicates that an impurity level of Zn^{2+} was capable of activating GaN enough to have high photocatalytic activity for overall water splitting. The photocatalyst activation is interesting, since a phenomenon is scarcely known that a small amount of dopants is able to enormously enhance the photocatalytic activity. The size of ion radii for Zn^{2+} was 0.074 nm for four coordination, whereas that for Mg^{2+} was 0.063 nm. The size of Mg^{2+} was smaller by 15% than that of Zn^{2+}, and it is plausible that similar or slightly larger amounts of Mg^{2+} ion were involved in Mg^{2+}-doped GaN.

As shown in photoluminescence spectra (Fig. 6), undoped GaN had emission at 373 nm, which was nearly the same as the band gap. The emission was assigned to electron transfer from the conduction to the valence band. On the other hand, the band-gap type emission for Mg^{2+}-doped GaN disappeared, and instead a strong broad emission appeared. The emission had a maximum at around 450 nm and a tail extending to a wavelength of 600 nm. For Zn^{2+}, Mg^{2+} and Be^{2+}-doped thin GaN films deposited on a sapphire substrate, the broad emission bands were reported to appear at 2.87, 2.95 and 2.2 eV at 2 K, respectively. The photoluminescence was explained in terms of a simple free to bound mechanism, i.e., transfer of free electrons at conduction bands to the acceptor levels of Zn_{Ga}, Mg_{Ga} and Be_{Ga} produced by doping of Zn^{2+}, Mg^{2+} and Be^{2+} to GaN, respectively [20,21]. The acceptor levels, Zn_{Ga}, Mg_{Ga} and Be_{Ga} were calculated to be higher by 0.34, 0.25, and 0.7 eV above the edge of valence band. The emission peaks observed in Zn^{2+}- and Mg^{2+}-doped GaN in the present study were nearly the same to the reported band emissions [20,21], and thus the photoluminescence by Zn^{2+}- and Mg^{2+}-doped GaN powder are associated with transfer of electrons from the conduction band/donor levels to acceptor levels, Zn_{Ga} and Mg_{Ga}, formed in the forbidden band. The electronic conditions indicate that GaN converted to p-type GaN by doping of Zn^{2+} and Mg^{2+}.

A series of studies on photocatalysis by typical metal oxides with d^{10} electronic configuration showed that the conduction bands are formed by hybridized sp orbitals with large band dispersion, indicative of high electron mobility. This indicates that d^{10} electronic configuration is advantageous for the

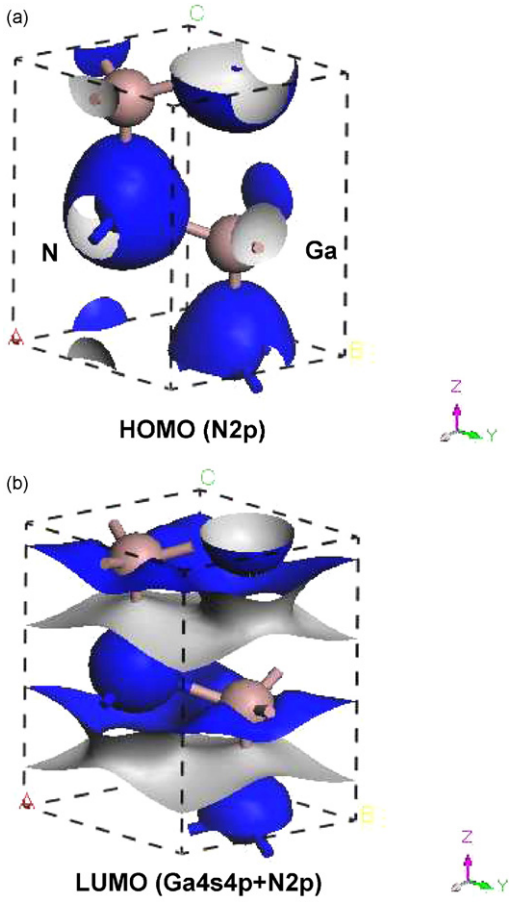

Fig. 8. Contour maps of HOMO (a) and LUMO (b) of GaN.

behavior of photoexcited electrons. The DFT calculation for GaN showed that the LUMO level of conduction band was composed of the hybridized Ga4s4p orbitals mixed with N2p orbital. Thus, the photoexcited electrons have large mobility to enable GaN to function as a photocatalyst. The doping of Si^{4+} and Ge^{4+} to GaN is known to produce donor levels, indicating of n-type GaN formation. As reported previously, however, tetravalent Si^{4+} and Ge^{4+} ion-doped GaN produced little H_2 and O_2 under similar reaction conditions, exhibiting no improvement of photocatalytic performance of GaN. This indicates that the situation of electrons is satisfactory to be photocatalytically active. Thus, a problem for poor ability of GaN is considered to be in the valence band, since it consisted of N2p orbital. The fact that the formation of p-type GaN by doping of the divalent metal ions is responsible for photocatalysis indicates the importance of hole control in photocatalytic water splitting by GaN. The appearance of strong photoluminescence indicated that the doping remarkably increased the conductivity due to hole. Thus, the high activity was associated with increasing hole concentrations due to the acceptor level formation.

With increasing Mg content in the mixture used in preparation, the intensity of emission of Mg^{2+}-doped GaN decreased monotonously, accompanied by a red shift of center position of the emission bands. The photoluminescence became negligible at Mg/(Mg + Ga) = 0.07. Meanwhile, the photocatalytic activity increased, attained a maximum level at around Mg/(Mg + Ga) = 0.05, and sharply decreased at Mg/(Mg + Ga) = 0.07. Thus, a change in photoluminescence intensity was opposite to that in photocatalytic activity, while both photoluminescence and activity disappeared at largest Mg content. Photoluminescence depends on various factors such as the density of photoexcited charges, the extent of non-radiation process, the mobility of photoexcited charges, and the density of recombination center. It is difficult to determine which process is mainly responsible for changes in photoluminescence intensity with Mg content. However, in comparison with photocatalytic activity changes, a plausible model is that an increase in Mg content enhanced the density of the acceptor levels and increased the concentration of holes and their mobility. The red shift of center position of photoluminescence peak indicates that with increasing Mg content the acceptor level is raised. This is related to the enhancement of photocatalytic activity because of strengthening of p-type properties. In the UV–vis diffuse reflectance spectra of undoped GaN and doped GaN, the absorption threshold of doped GaN slightly shifted to longer wavelength, compared to that of undoped GaN, although absorption maximum remained unchanged. The shift resulted from absorption increase at around 400–450 nm, which is likely to be due to the formation of defects. Thus, a large amount of Mg increased the density of defects, which weakens the photoluminescence and lowers photocatalytic activity. Changes in the intensity of 1 0 0 and 1 0 2 peaks (Fig. 4) are likely to be an indication that Zn^{2+} and Mg^{2+}-doping affected the crystal structures of GaN.

In n- or p-type GaN thin film photoelectrode deposited on a sapphire substrate grown by metalorganic vapor-phase epitaxy, H_2 and a trace amount of O_2, together with a considerable amount of N_2, were reported to be produced from H_2O by UV irradiation under an applied voltage of +1.0 V[22,23]. In present study, divalent metal ion (Zn^{2+}, Mg^{2+} or Be^{2+})-doped GaN powder combined with RuO_2 showed high and stable water splitting with the stoichiometric ratio without an external force. Various p-block metal oxides such as MGa_2O_4 (M = Sr, Ba, Zn), MIn_2O_4 (M = Ca, Sr), Zn_2GeO_4, M_2SnO_4 (M = Ca, Sr), $NaSbO_3$ and $M_2Sb_2O_7$ (M = Ca, Sr) became effective photocatalysts for water splitting when combined with RuO_2. The activity dependence of preparation temperatures demonstrated that the activity increased with increasing temperature, passed through a maximum and decreased. Such changes were explained in terms of the view that activity enhancement was associated with the crystallization of metal oxides formed, whereas activity decrease was caused by the agglomeration of RuO_2 particles, indicative of the importance of dispersion of RuO_2 on the metal oxide surfaces to achieve high photocatalytic performance. Thus, photocatalysis by RuO_2-dispersed doped GaN without an external force is due to the combination of highly crystallized GaN with dispersed RuO_2 as a co-catalyst.

5. Conclusion

The divalent metal ions (Zn^{2+}, Mg^{2+} and Be^{2+}) doped p-type GaN with d^{10} electronic configuration became active photocatalysts, when combined with RuO_2, for overall water splitting

to stoichiometrically produce hydrogen and oxygen. The activation was concluded to be due to the formation of p-type GaN with the acceptor levels above valence bands, which improves the behavior of holes.

Acknowledgements

This work was supported by the Solution Oriented Research for Science and Technology (SORST) and the Core Research for Evolution Science and Technology (CREST) program of the Japan Science and Technology (JST) Corporation, and funded by a Grant-in-Aid for Scientific Research in Priority Areas (17029022) from The Ministry of Education, Culture, Sports, Science and Technology of Japan.

References

[1] T. Takata, K. Shinohara, A. Tanaka, M. Hara, J. Kondo, K. Domen, J. Photochem. Photobiol. A 106 (1997) 45.
[2] Y. Inoue, T. Kubokawa, K. Sato, J. Phys. Chem. 95 (1991) 4059.
[3] Y. Inoue, Y. Asai, K. Sato, J. Chem. Soc. Faraday Trans. 90 (1994) 979.
[4] A. Kudo, A. Tanaka, K. Domen, K. Maruya, K. Aika, T. Onishi, J. Catal. 111 (1998) 67.
[5] K. Sayama, H. Arakawa, J. Phys. Chem. 97 (1993) 531.
[6] H. Kato, K. Asakura, A. Kudo, J. Am. Chem. Soc. 125 (2003) 3082.
[7] K. Domen, J. Kondo, M. Hara, T. Takata, Bull. Chem. Soc. Jpn. 73 (2000) 1307.
[8] N. Saito, H. Kadowaki, H. Kobayashi, K. Ikarashi, H. Nishiyama, Y. Inoue, Chem. Lett. 33 (2004) 33.
[9] K. Ikarashi, J. Sato, N. Saito, H. Kobayashi, H. Nishiyama, Y. Inoue, J. Phys. Chem. B 106 (2002) 9048.
[10] J. Sato, N. Saito, H. Nishiyama, Y. Inoue, J. Phys. Chem. B 107 (2003) 7965.
[11] J. Sato, H. Kobayashi, K. Ikarashi, N. Saito, H. Nishiyama, Y. Inoue, J. Phys. Chem. B 108 (2004) 4369.
[12] J. Sato, H. Kobayashi, Y. Inoue, J. Phys. Chem. B 107 (2003) 7970.
[13] J. Sato, N. Saito, H. Nishiyama, Y. Inoue, J. Phys. Chem. B 105 (2001) 6061.
[14] J. Sato, H. Koboyashi, N. Saito, H. Nishiyama, Y. Inoue, J. Photochem. Photobiol. A 158 (2003) 139.
[15] H. Kadowaki, N. Saito, H. Nishiyama, Y. Inoue, J. Phys. Chem. B 109 (2005) 22995.
[16] J. Sato, N. Saito, Y. Yamada, K. Maeda, T. Takata, J.N. Kondo, M. Hara, H. Kobayashi, K. Domen, Y. Inoue, J. Am. Chem. Soc. 127 (2005) 4150.
[17] N. Arai, N. Saito, H. Nishiyama, Y. Inoue, K. Domen, K. Sato, Chem. Lett. 35 (2006) 796.
[18] K. Maeda, T. Takata, M. Hara, N. Saito, Y. Inoue, H. Kobayashi, K. Domen, J. Am. Chem. Soc. 127 (2005) 8286.
[19] K. Maeda, K. Teramura, D. Lu, T. Takata, N. Saito, Y. Inoue, K. Domen, Nature 440 (2006) 295.
[20] P. Bergman, G. Ying, B. Monemar, P.O. Holtz, J. Appl. Phys. 61 (1987) 4589.
[21] B. Monemar, J.P. Bergman, I.A. Buyanova, in: M.O. Manasreh (Ed.), Optoelecronic Properties of Semiconductors and Superlattices, vol. 2, Gordon and Breach Science Publishers, Amsterdam, 1997„ p. 85Chap. 4.
[22] K. Fujii, K. Kusakabe, K. Ohkawa, Jpn. J. Appl. Phys. 44 (2005) 7433.
[23] K. Fujii, K. Ohkawa, Jpn. J. Appl. Phys. 44 (2005) L909.